applied optics

Radiometric calibration method for large aperture infrared system with broad dynamic range

ZHIYUAN SUN,[1,*] SONGTAO CHANG,[1,2] AND WEI ZHU[1]

[1]Changchun Institute of Optics, Fine Mechanics and Physics, Chinese Academy of Sciences, Changchun 130033, China
[2]University of Chinese Academy of Sciences, Beijing 100039, China
*Corresponding author: zhiyuansun2011@hotmail.com

Received 30 January 2015; revised 22 April 2015; accepted 23 April 2015; posted 23 April 2015 (Doc. ID 233549); published 12 May 2015

Infrared radiometric measurements can acquire important data for missile defense systems. When observation is carried out by ground-based infrared systems, a missile is characterized by long distance, small size, and large variation of radiance. Therefore, the infrared systems should be manufactured with a larger aperture to enhance detection ability and calibrated at a broader dynamic range to extend measurable radiance. Nevertheless, the frequently used calibration methods demand an extended-area blackbody with broad dynamic range or a huge collimator for filling the system's field stop, which would greatly increase manufacturing costs and difficulties. To overcome this restriction, a calibration method based on amendment of inner and outer calibration is proposed. First, the principles and procedures of this method are introduced. Then, a shifting strategy of infrared systems for measuring targets with large fluctuations of infrared radiance is put forward. Finally, several experiments are performed on a shortwave infrared system with Φ400 mm aperture. The results indicate that the proposed method cannot only ensure accuracy of calibration but have the advantage of low cost, low power, and high motility. Hence, it is an effective radiometric calibration method in the outfield.

OCIS codes: (010.5630) Radiometry; (040.2480) FLIR, forward-looking infrared; (040.3060) Infrared; (120.0280) Remote sensing and sensors.

http://dx.doi.org/10.1364/AO.54.004659

1. INTRODUCTION

With the development of infrared detectors and radiometry technology, ground-based infrared imaging systems are often widely used to measure radiometric characteristics of military and scientific objects. Apparently, when targets with a very large variation range of infrared radiation are detected, it is vital that infrared systems have the same broad dynamic range to detect overall information of the targets. Therefore, several different integration times [1,2] are selected to avoid saturation of the detector, and infrared neutral filters are added into infrared systems in some cases. On the other hand, in order to acquire the radiation distribution rather than an average radiance of targets, the ground-based infrared systems should be designed to have a large aperture to increase the image size. As a consequence, it is meaningful to study the calibration method of large aperture ground-based infrared systems with broad dynamic range.

There exist numerous calibration configurations for different infrared systems, and the approaches that are commonly used on large aperture ground-based infrared system are briefly classified into three categories. (1) An extended area blackbody is placed directly in front of the infrared system for calibration, namely, near-extended-source (NES) configuration [3,4]. Radiation from the blackbody (out of focus) completely fills the field stop. This method yields high calibration accuracy because there is no background and minimal atmosphere, whereas its drawbacks reside in the fact that the extended area blackbody with high temperature will greatly enhance the costs and manufacturing difficulties, so it tends to become inadaptable for broad dynamic range radiometric calibration. (2) A small source is placed at the focal point of a collimator and the image of source should fill likewise the field stop. This method is named as the near collimating optics configuration [3,5]; one can use a small source to obtain a large area radiometric signal, but the collimator hardware can be expensive and may be restrictive in a laboratory setting. (3) Infrared stars calibration configuration [6–8] is practical for outfield calibration because many infrared stars exists, and their output is sufficiently known. However, precision cannot be guaranteed due to the typical small signals and the effect of atmosphere.

In this article, radiometric calibration formulas considering the integration time and transmissivity of neutral attenuator are proposed, and the effective gray value range of the infrared detector when calibrating is analyzed in Section 2. Following this,

a calibration method based on the amendment of inner and outer calibration is proposed in Section 3. In Section 4, calibration experiments based on a shortwave infrared (SWIR) system with Φ400 mm diameter are carried out to acquire calibration data, from which an optimized strategy is extracted to handle the targets with large variation of radiance. Afterward, an extended-area blackbody placed on the focal point of an off-axis collimator is regarded as the target to verify the method and strategy described above. It is concluded in Section 5 that our method yields high precision while performing broad dynamic range radiometric calibration on a large aperture infrared system. Besides, it cuts the costs and provides users with a feasible calibration method in the outfield.

2. RADIOMETRIC CALIBRATION

A. Radiometric Calibration Considering the Integration Time and Transmissivity of Neutral Filter

Radiometric calibration of an infrared imaging system is essential to properly determine the target's radiance or temperature. The NES radiometric calibration is a commonly used calibration configuration, which is shown in Fig. 1.

The output gray value (DN, digital number) is given by the approximate linear relation [9–11]:

$$h_{i,j} = t \cdot S_{i,j} \cdot \Phi_t + B_{i,j}, \tag{1}$$

where $h_{i,j}$ is the gray value of the (i,j)th detector element in the array, t is the integration time in units of ms, $S_{i,j}$ is the response associated with incident flux of the reference source, and $B_{i,j}$ is the offset. The radiation flux Φ_t can be calculated by

$$\Phi_t = \frac{\pi \cdot \varepsilon \cdot \tau_{\text{opt}}}{4} \cdot \left(\frac{D}{f}\right)^2 \cdot A_d \cdot L(T_t) = \varepsilon \cdot k_t \cdot L(T_t), \tag{2}$$

where ε denotes the emissivity of the reference source, τ_{opt} denotes transmissivity of the optics, D is diameter of the optics, f is the focal length, A_d is sensitive area of a detector element, $L(T_t)$ denotes the in-band radiance of an ideal blackbody at absolute temperature T_t, and $k_t = \frac{\pi \cdot \tau_{\text{opt}}}{4} \cdot (\frac{D}{f})^2 \cdot A_d$ is constant for a given infrared system.

The offset $B_{i,j}$, originating from the reflected ambient radiation, scattered radiation, and internal factors of the detector (for instance, dark current), which strike the detector element, is given by

$$B_{i,j} = t \cdot S_{i,j} \cdot \Phi_{\text{stray},i,j} + h_{\text{det},i,j}, \tag{3}$$

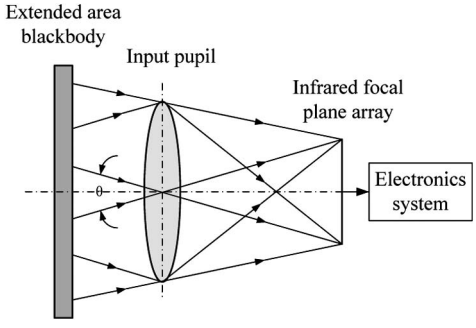

Fig. 1. Diagram of NES radiometric calibration configuration.

where $\Phi_{\text{stray},i,j}$ is the stray radiation flux, which consists of the reflected ambient radiation flux and the scattered radiation flux, and $h_{\text{det},i,j}$ is the gray value offset caused by internal factors of the detector.

The response of a detector element to radiance is given by $G_{i,j} = S_{i,j} \cdot k_t$, and then Eq. (1) can be rewritten as

$$h_{i,j} = t \cdot G_{i,j} \cdot \varepsilon \cdot L(T_t) + t \cdot G_{i,j} \cdot L_{\text{stray},i,j} + h_{\text{det},i,j}, \tag{4}$$

where $L_{\text{stray},i,j}$ is the corresponding radiance, which arouses $\Phi_{\text{stray},i,j}$.

In order to meet broad dynamic range requirements of imaging as well as radiometry applications, infrared neutral filters are added in the infrared system. Of course, the incident radiation flux, which falls into the linear range of detector response, is reduced, as long as the transmissivity of neutral filters is less than 1. Ignoring the index of the detector element above, the calibration formula Eq. (4) can be rewritten as

$$h = t \cdot \tau_{\text{filter}} \cdot G \cdot \varepsilon \cdot L(T_t) + t \cdot G \cdot L_{\text{stray}} + h_{\text{det}}, \tag{5}$$

where τ_{filter} is the mean transmissivity of neutral filter at the response waveband of the infrared detector; G, therefore, is redefined as the normalized radiance response in units of $\text{DN}/(\text{ms} \cdot \text{W} \cdot \text{m}^{-2} \cdot \text{sr}^{-1})$. It is noticed that, for the NES calibration method, the reference source is so close to the detector that the atmospheric effects, namely, absorption and scattering, can be ignored.

When employing a stable blackbody to calibrate an infrared system, G, L_{stray}, and h_{det} are unknown coefficients, which can be determined by calibration data.

B. Effective Gray Value Range for Calibrating

When operating in a range of radiance within which detectors exhibit linear input–output characteristics, the infrared systems possess favorable radiometry precision. Due to this, the effective gray value range should be analyzed when providing the signal-to-noise ratio (SNR).

The first term in Eq. (5), which contains the radiance of reference blackbody, represents the signal. L_{stray} is a variable relative to ambient temperature and system structure, so the second term is regarded as the noise of radiometric calibration. For a cooled infrared system, where the temperature of the detector elements keeps nearly constant (i.e., 77 K), h_{det} is assumed constant in the process of calibration. The SNR for radiometric calibration is expressed as

$$\text{SNR}_{\text{calibration}} = \frac{t \cdot \tau_{\text{filter}} \cdot G \cdot \varepsilon \cdot L(T_t)}{t \cdot G \cdot L_{\text{stray}}} = \frac{\tau_{\text{filter}} \cdot \varepsilon \cdot L(T_t)}{L_{\text{stray}}}. \tag{6}$$

Obviously, if the temperature of the blackbody is set to a small value, or a filter with high attenuation is shifted into the optical path, the SNR is small. In order to enhance the precision of radiometric calibration, the SNR should be larger than 1. So the minimal gray value can be expressed as

$$h_{\min} > 2 \cdot t \cdot G \cdot L_{\text{stray}} + h_{\text{det}}, \tag{7}$$

where $h_{\min}$ could be calculated after the calibration formula is determined. It is noted that the effective gray value range for calibration should be restricted between $h_{\min}$ and the saturated gray value.

3. CALIBRATION METHOD BASED ON AMENDMENT OF INNER AND OUTER CALIBRATION

The scheme of radiometric calibration method based on amendment of inner and outer calibration is shown in Fig. 2. A cavity blackbody is located on the equivalent position of the first image plane in the optical system. The radiation of the cavity blackbody could be introduced to or removed from the optical system by shifting the switching reflector. When the switching reflector remains in the optical path, the configuration is the outer calibration when the whole optical system is calibrated at a narrow temperature scope by virtue of a general extended area blackbody. On the contrary, the configuration is the inner calibration if the switching reflector is shifted out, and the partial optical system images the cavity blackbody onto the infrared detector. It is confirmed that the cavity blackbody fills the field of the partial optical system by particular optical designs. Therefore, the broad dynamic range calibration data of the partial optical system are gained. The relationship between inner and outer calibration can be calculated by the calibration data at a communal temperature range. After amending, broad dynamic range calibration results of the whole system could be acquired.

When the outer calibration is carried out, the whole optical system is calibrated by the extended area blackbody; the output gray value of detector is given by

$$h = t \cdot \tau_{\text{filter}} \cdot G_w \cdot \varepsilon_w \cdot L(T_t) + t \cdot G_w \cdot L_{\text{stray},w} + h_{\text{det},w}, \quad (8)$$

where h is the output gray value of the detector element, t is the integration time, τ_{filter} is the transmissivity of the neutral filter, G_w is the response of a detector element to radiance in the outer calibration configuration, ε_w is the emissivity of the extended area blackbody, $L_{\text{stray},w}$ is the stray radiance caused by reflected ambient radiance and scattered radiance when processing outer calibration, and $h_{\text{det},w}$ is the gray value offset caused by internal factors of the detector.

When processing the inner calibration, the cavity blackbody fills the field of the posterior optical system at a close distance; therefore, the calibration is also NES configuration. The partial optical system is calibrated by the cavity blackbody, and the output gray value of the detector is given by

$$h = t \cdot \tau_{\text{filter}} \cdot G_n \cdot \varepsilon_n \cdot L(T_t) + t \cdot G_n \cdot L_{\text{stray},n} + h_{\text{det},n}, \quad (9)$$

where h is the output gray value of the detector, t is the integration time, τ_{filter} is the transmissivity of the neutral filter, G_n is the response of a detector element to radiance in the inner calibration configuration, ε_n is the emissivity of the cavity blackbody, and $L_{\text{stray},n}$ is the stray radiance caused by reflected ambient radiance and scattered radiance when processing inner calibration. $h_{\text{det},n}$ is the gray value offset caused by internal factors of the detector.

In contrast with inner calibration, outer calibration occupies more lenses, including primary reflector, dichroic lens 1, dichroic lens 2, secondary reflector, sealing lens, and switching reflector. The six lenses mentioned above could be regarded as a unity, which is nominated as the fore system. Based on the inner calibration expression, the outer calibration could be expressed in another format:

$$\begin{aligned} h &= t \cdot \tau_{\text{filter}} \cdot G_n \cdot (\tau_{\text{ps}} \cdot \varepsilon_w \cdot L(T_t) + B_{\text{ps}}) \\ &\quad + t \cdot G_n \cdot L_{\text{stray},n} + h_{\text{det},n} \\ &= t \cdot \tau_{\text{filter}} \cdot G_n \cdot \tau_{\text{ps}} \cdot \varepsilon_w \cdot L(T_t) \\ &\quad + t \cdot \tau_{\text{filter}} \cdot G_n \cdot B_{\text{ps}} + t \cdot G_n \cdot L_{\text{stray},n} + h_{\text{det},n}, \end{aligned} \quad (10)$$

where τ_{ps} and B_{ps} are, respectively, the attenuation rate and offset of the fore system.

The following equivalent equations could be deduced owing to the simultaneous equations of Eqs. (8) and (10):

$$t \cdot \tau_{\text{filter}} \cdot G_w \cdot \varepsilon_w = t \cdot \tau_{\text{filter}} \cdot G_n \cdot \tau_{\text{ps}} \cdot \varepsilon_w, \quad (11)$$

$$\begin{aligned} &t \cdot G_w \cdot L_{\text{stray},w} + h_{\text{det},w} \\ &\quad = t \cdot \tau_{\text{filter}} \cdot G_n \cdot B_{\text{ps}} + t \cdot G_n \cdot L_{\text{stray},n} + h_{\text{det},n}. \end{aligned} \quad (12)$$

Equations (11) and (12) could be simplified as

$$\tau_{\text{ps}} = \frac{G_w}{G_n}, \quad (13)$$

$$B_{\text{ps}} = \frac{t(G_w \cdot L_{\text{stray},w} - G_n \cdot L_{\text{stray},n}) + (h_{\text{det},w} - h_{\text{det},n})}{t \cdot \tau_{\text{filter}} \cdot G_n}. \quad (14)$$

For a cooled infrared system, where temperature of the detector elements keeps almost constant, h_{det} is approximately assumed as a constant. Equation (14) can be rewritten as

$$B_{\text{ps}} = \frac{G_w \cdot L_{\text{stray},w} - G_n \cdot L_{\text{stray},n}}{\tau_{\text{filter}} \cdot G_n}. \quad (15)$$

Calibration data of the communal temperature range are chosen from the outer and inner calibrations to calculate respective parameters (G_w, $L_{\text{stray},w}$, G_n, and $L_{\text{stray},n}$) in the calibration formula. Afterward, τ_{ps} and B_{ps} could be calculated.

As shown in Eq. (9), taking $L(T_t)$ as an independent variable and h as dependent variable accordingly, $A = t \cdot \tau_{\text{filter}} \cdot G_n \cdot \varepsilon_n$ and $B = t \cdot G_n \cdot L_{\text{stray},n} + h_{\text{det}}$, which denote the slope and offset of the inner calibration formula at broad temperature range can be calculated afterward. Employing τ_{ps} and B_{ps} to amend the inner calibration data, the calibration data of the

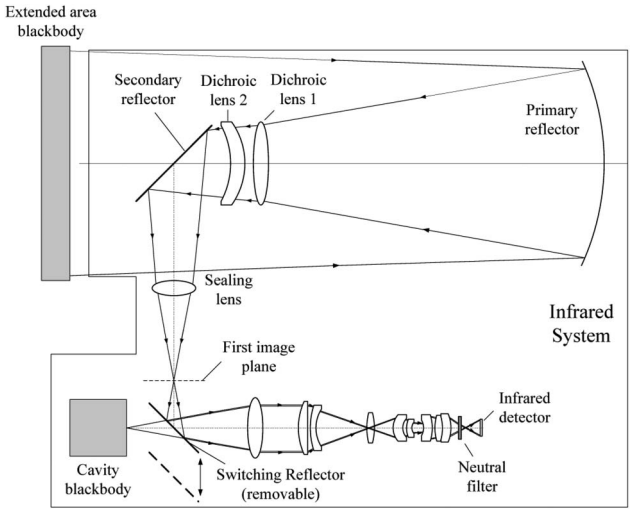

Fig. 2. Scheme of calibration method based on amendment of inner and outer calibration.

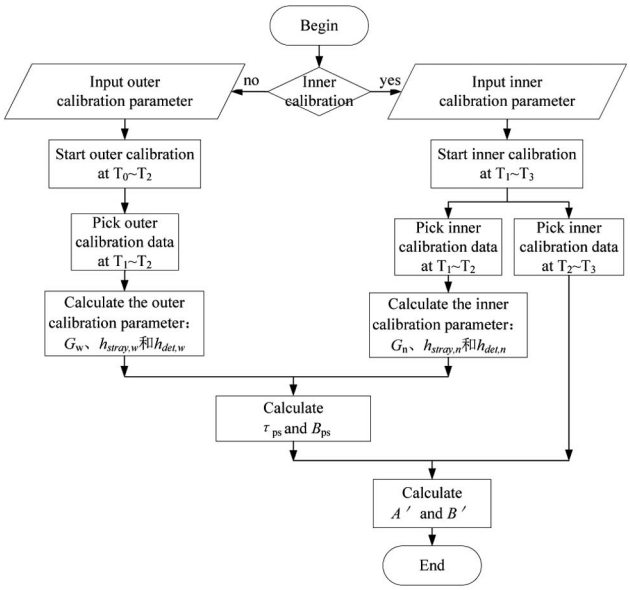

Fig. 3. Flow chart of radiometric calibration process. $T_0 \sim T_2$ and $T_1 \sim T_3$ are, respectively, the temperature ranges of inner calibration and outer calibration.

whole system at broad dynamic range, which goes beyond the limit of the extended area blackbody, could be obtained. The calibration formula of the whole system can be expressed as

$$h = A' \cdot L(T_t) + B', \tag{16}$$

where $A' = A \cdot \tau_{ps}$ and $B' = B + t \cdot \tau_{filter} \cdot G_n \cdot B_{ps}$ separately denote the slope and offset in calibration formula of the whole system at a broad dynamic range. A flow chart of the calibration is illustrated in Fig. 3.

$T_1 \sim T_2$ represents communal temperature range of outer and inner calibration.

4. EXPERIMENTAL RESULTS

A. Experimental Setup

To verify the radiometric calibration method described above, experiments were performed on a SWIR system having a large-scale FPA (320 × 256 pixels). The aperture of the system is Φ400 mm, and the focal length is 800 mm. The FPA operates in 0.8–2.5 μm waveband, with a 14 bit digital output. In order to increase the SWIR system's dynamic range, one of the four neutral filters mounted on the filter wheel should be switched into the optical path to reduce the incident radiation. The mean transmissivity of the neutral filters at the response waveband of the infrared detector are 100%, 20%, 5%, and 2%, respectively.

The SR200 cavity blackbody manufactured by CI Systems, selected as the inner calibration blackbody, has a Φ1 in. size (1 in. = 2.54 cm) and exhibits high effective emissivity (0.99 in 0.8–2.5 μm waveband). Its temperature accuracy is 0.3% over the operating temperature range of 50°C–1200°C.

B. Results of Outer Calibration

The SR800-20A extended-area blackbody manufactured by CI Systems is adopted to calibrate the SWIR system. The blackbody has a 20 in. × 20 in. (508 mm × 508 mm) size and exhibits high effective emissivity (0.97 in 0.8–2.5 μm waveband). Its temperature accuracy is 0.01°C over an operating temperature range of 0°C–125°C. Because of the excellent response linearity of the detector array, it is not essential to calibrate at each temperature point. Furthermore, given the temperature range of the inner cavity blackbody, the temperature range of outer calibration is chosen as 100°C–150°C with an interval of 5°C.

According to Eq. (7), the lower transmissivity of the neutral filter and the smaller integration time will lead to unsatisfactory linearity of the calibration curve; therefore, the calculation precision of G, L_{stray}, and h_{det} will be affected as a result. For this reason, 140°C and 150°C at 100% neutral filter configuration are chosen to calculate the undetermined coefficients of the outer calibration formula. Result of the coefficients in the outer calibration formula is listed in Table 1.

According to L_{stray} and h_{det} shown in Table 1, the minimal gray value calculated by Eq. (7) is listed in Table 2.

Figure 4 shows the outer calibration results at several integration times when the transmissivity of neutral filters are 100% and 2%, respectively.

As shown in Fig. 4(a), when the transmissivity of the neutral filter is 100%, fewer calibration points drop out of the effective gray value range, which is determined by the minimal gray value and saturated gray value. Therefore, the calibration curve can be accurately fitted by the least-squares method. However, if the transmissivity of the neutral filter is 2%, no calibration points are inside the demanding gray value range, as is shown in Fig. 4(b). This indicates that the small SNR, caused by low transmissivity, can destroy the linearity of the response curve, and the precision of radiometric calibration is influenced as a result. Thus, the inner calibration is necessary for those infrared systems requiring broad dynamic range.

C. Calibration Results of Whole System Calculated By Inner Calibration

In order to ensure the communal temperature range, the temperature of inner calibration is selected from 100°C at intervals of 10°C. Figure 5 shows the inner calibration results at several integration times when the transmissivity of neutral filters is 100% and 2%, respectively.

Table 1. Coefficients of Outer Calibration Formula

Calibration Model	G_w (DN/(ms · W · m^{-2} · sr^{-1}))	$L_{stray,w}$ (W · m^{-2} · sr^{-1})	$h_{det,w}$ (DN)
Outer calibration	1633.8	0.1027	1795.5

Table 2. Minimal Gray Value Required at Different Integration Times

Integration Time (ms)	h_{min} (DN)
4	3138
0.76	2051
0.12	1836

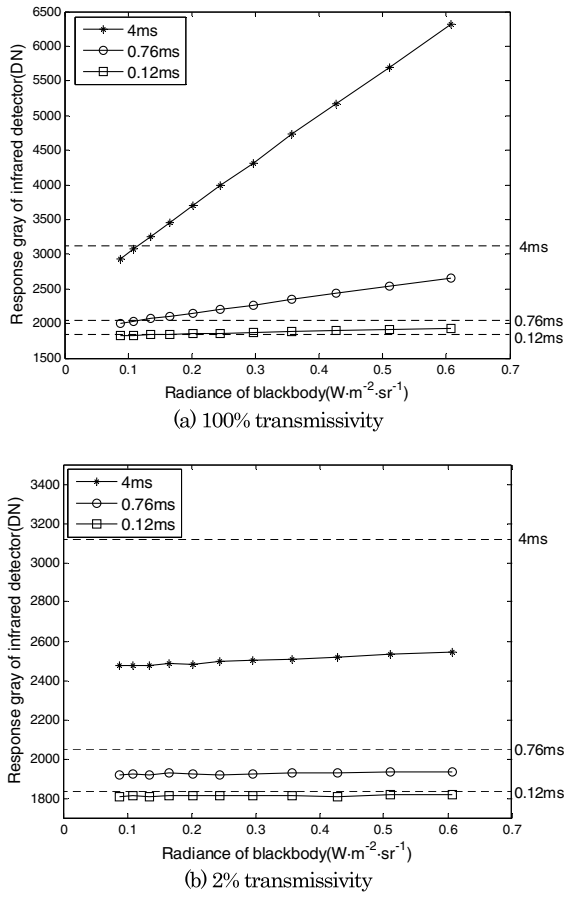

Fig. 4. (a) and (b) Outer calibration results at several integration times when the transmissivity of neutral filters is 100% and 2%, respectively. The dashed line represents the minimal gray value at the special integration time labeled on the right side. The x axis is the corresponding radiance of blackbody from 100°C to 150°C at intervals of 5°C, and the leftmost y axis is the gray value of infrared detector.

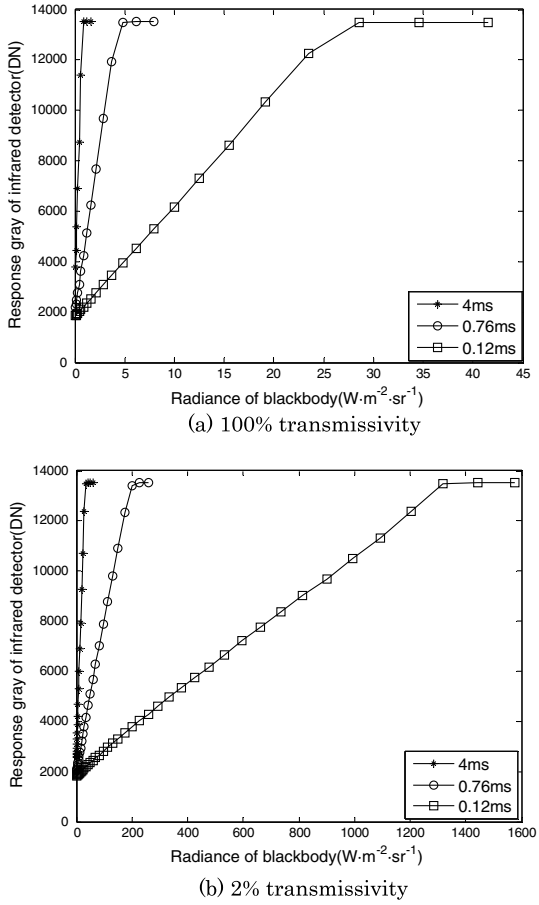

Fig. 5. (a) and (b) Inner calibration results at several integration times when transmissivity of the neutral filter is 100% and 2%, respectively. The x axis is the corresponding radiance of the blackbody from 100°C at intervals of 10°C, and the leftmost y axis is the gray value of the infrared detector.

As shown in Fig. 5(a), when the transmissivity of the neutral filter is 100%, the saturated temperatures are 160°C, 220°C, and 300°C on the condition that integration times are 4, 0.76, and 0.12 ms, correspondingly. Furthermore, the saturated temperatures are 310°C, 420°C, and 590°C at the three integration times when switching a neutral filter to 2% transmissivity.

It is illustrated in Fig. 5 that the larger the integration time, the smaller the saturated temperature. If the temperature of the blackbody exceeds the saturated temperature, the gray value of the detector will remain constant at about 13500, instead of increasing continuously. Hence, the saturated calibration points should be excluded when fitting calibration curves.

The inner calibration data at the same temperature range as outer calibration are employed to calculate the undetermined coefficients. The results are shown in Table 3.

As shown in Tables 1 and 3, $L_{\text{stray},w}$ and $L_{\text{stray},n}$ are not equal. However, $h_{\text{det},w}$ and $h_{\text{det},n}$, which represent the internal factors of the detector element, are approximatively equal, which verifies the assumption in Eq. (14).

The minimal gray value of different integration times in the inner calibration configuration could be calculated by Eq. (7). First, the calibration points dropping out of the effective gray value range are picked out. Then, the calibration points with larger residual errors are eliminated by regression analysis. Finally, the remnant calibration points could be applied to fit the inner calibration formula by means of the least-squares method.

The coefficients of calibration formulas listed in Tables 1 and 3 are placed into Eqs. (13) and (15); the attenuation rate (τ_{ps}) and the offset of fore system (B_{ps}) could be calculated. Afterward, the calibration formulas of the whole system could be deduced with the help of Eq. (16). The calibration formulas of the whole system and the corresponding inner calibration formulas are listed in Table 4.

D. Combination of Calibration Data to Measure Broad Dynamic Range Target

Since the calibration formulas of the whole system calculated by inner calibration contain some errors on account of blackbody differences, amendment errors, and fitting errors, the outer calibration data and the whole system data calculated by inner calibration should be combined to calculate the radiance of the target with broad dynamic range.

Table 3. Coefficients of Inner Calibration Formula

Calibration Model	G_n (DN/(ms · W · m^{-2} · sr^{-1}))	$L_{\text{stray},n}$ (W · m^{-2} · sr^{-1})	$b_{\text{det},n}$ (DN)
Inner calibration	3763.9	0.0371	1796.5

When the target first comes into sight, the radiance projected on the infrared system is small, so the largest integration time and the neutral filter with 100% transmissivity should be employed in the infrared system for ensuring the max gray value on the detector element to easily seize the target. In this period, outer calibration data are applied to measure radiance of the target. With the target gets near, the radiance increases rapidly, the integration time should be decreased to avoid saturation. However, if the gray value of the detector element comes to saturation, even when the integration time has been set to the minimum, the neutral filter has to be shifted. But the target's gray may jump out of the linear scope in case of using outer calibration data, which would not guarantee the calibration precision. As a result, the calibration data of the whole system calculated by inner calibration come into use.

The whole system's calibration formulas calculated by inner calibration are shown in Table 4. Not all the integration times and all the neutral filters have to be used in the measurement. One should choose a suitable shifting strategy, based on which gray value of the target could be maintained in the linear scope of the detector during the whole flight, despite the fluctuation of radiance. The essential rules for determining the strategy are as follows:

1. Least changes or switches should be carried out, and the change of integration time should be prior to the switch of the neutral filter because of the extremely short alteration time.

2. It is confirmed that the gray values of the target are in the linear scope of the detector to maintain good SNR. Referring to the effective gray value range for calibration introduced in Section 2.B, 3500 is defined as the minimum gray value for measuring. Meanwhile, because the saturated gray value of detector is 13,500, 13,000 is regarded as the maximum gray value after adding a safety factor.

According to the rules referred to above, the calibration results are rearranged, and several calibration results are picked out to form a strategy for measurement, which is shown in Table 5. With the combination of integration time and if a neutral filter is regarded as a shifting gear, then there are five gears in the strategy (symbols of these gears are listed in Table 5).

Figure 6 simulates the gray value variation progress on the detector element, while the target radiance increases gradually. At the beginning of observation, the gear is set to I. The target's radiance will increase as it gets near. When the radiance projected on the infrared system reaches 1.63 W/(m^2 · sr), the theoretical gray value of the detector element will get to 13,000. Then, the gear will shift to II by changing the integration time. Similarly, shifting from II to III could also be enforced by changing the integration time. However, integration time and the neutral filter should be simultaneously altered when shifting from III to IV.

I, II, and III gears are based on the outer calibration data, and the maximum measurable radiance is 54.92 W/(m^2 · sr). Meanwhile, IV and V gears are the whole system results calculated by the inner calibration data. The maximum measurable radiance is 2918.36 W/(m^2 · sr), which is about 53 times the radiance of not using inner calibration. It is notable that the maximum radiance refers to the radiance projected on the infrared system. The actual radiance of the target is greater in consideration of atmosphere absorption.

Table 4. Inner Calibration Formulas at Different Integration Times

Transmissivity of Neutral Filter (%)	Integration Time (ms)	Formula of Inner Calibration	Calibration Formula of the Whole System
20	0.12	$y = 104.14^*x + 1856.46$	$y = 45.20^*x + 1859.84$
	0.76	$y = 644.78^*x + 1949.22$	$y = 279.88^*x + 1970.61$
	4	$y = 3517.88^*x + 2525.82$	$y = 1527.01^*x + 2638.42$
5	0.12	$y = 23.18^*x + 1877.98$	$y = 10.06^*x + 1881.36$
	0.76	$y = 154.61^*x + 1950.66$	$y = 67.11^*x + 1972.05$
	4	$y = 820.48^*x + 2621.74$	$y = 356.15^*x + 2734.34$
2	0.12	$y = 8.71^*x + 1965.21$	$y = 3.78^*x + 1968.59$
	0.76	$y = 61.86^*x + 1980.77$	$y = 26.85^*x + 2002.16$
	4	$y = 346.91^*x + 2551.72$	$y = 150.58^*x + 2664.32$

Table 5. Calibration Results of the Whole System

Transmissivity of Neutral Filter (%)	Integration Time (ms)	Symbol of Gear	Calibration Formula of the Whole System
100	4	I	$y = 6503.28^*x + 2381.93$
	0.76	II	$y = 1245.04^*x + 1899.69$
	0.12	III	$y = 203.76^*x + 1809.71$
2	0.76	IV	$y = 26.85^*x + 2002.16$
	0.12	V	$y = 3.78^*x + 1968.59$

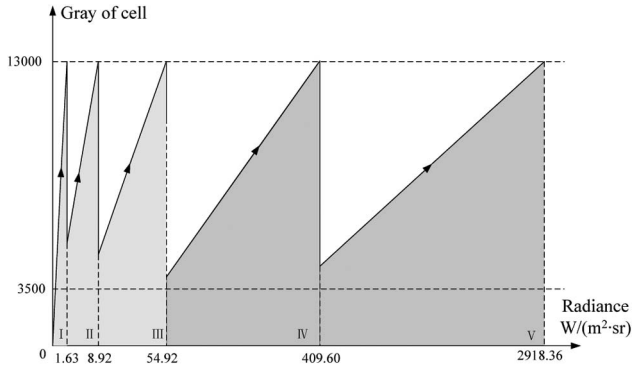

Fig. 6. Variation process of gray value on the detector while radiance of target increases gradually. The x axis is the radiance of the target projected on the entrance of infrared system. The y axis is the gray value of elements that the target occupies.

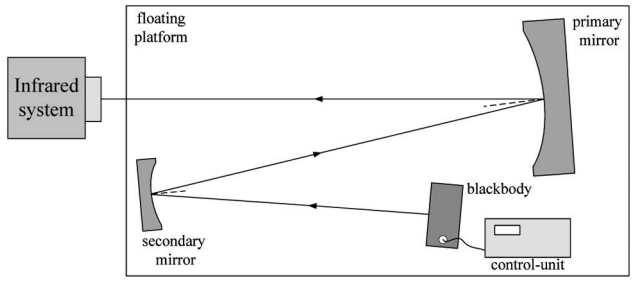

Fig. 7. Experimental setup for measurement.

E. Calibration Results of the Whole System and Inversion Precision

In order to inspect measurement precision of the calibration result listed in Table 5, an extended area blackbody was placed on the focal point of an off-axis collimator, and the blackbody radiation was expanded and collimated to act as the object (shown in Fig. 7).

The blackbody had a 12 in. × 12 in.. (about 304.8 mm) size and exhibited high effective emissivity (0.97 in 0.8–2.5 μm waveband). Its temperature accuracy was 0.1°C over an operating temperature range of 50°C–550°C. The collimator had a Φ600 mm size and operated at the infrared waveband. In order to simulate the radiance fluctuations, the blackbody temperatures are not set in order. The radiance has been calculated from the calibration formulas of Table 5, and the results can be seen in Table 6.

As shown in Table 6, maximal measurement error of radiance occurs at 480°C. The corresponding shifting gear is V at which the integration time and transmissivity are both at least value. Meanwhile, another temperature point 550°C trapped into gear V also displays low accuracy. Therefore, the worse radiance precisions of gear V are mainly caused by smaller SNR. But, for the other gears, the maximal error of radiance is 1.14%, and the shifting strategy ensures that gray values locate within the linear scope of detector.

5. CONCLUSION

This paper introduces an approach to calibrate a large aperture infrared system with a broad dynamic range. A cavity blackbody is mounted into the infrared system and imaged on the infrared detector through a special optical design. The partial optical system could be calibrated by the cavity blackbody at a broad dynamic range. Then, employing the correction factor between the partial system and the whole system to amend the inner calibration results referred above, the calibration results of the whole infrared system could be gained. Finally, calibration experiments are performed based on an SWIR system with Φ400 mm diameter to evaluate whether the method proposed is effective for a large aperture infrared system with broad dynamic range. Experimental results illustrate that the calibration method yields high precision of radiometric calibration.

The main advantage of the approach developed in this paper is the absence of a large aperture collimator when processing the radiometric calibration at a broad dynamic range, thus reducing costs and which is capable to be carried through in the outfield. What has to be pointed out is that the calibration results are relevant with the inner temperature of the infrared system. When calibration is taken though in the outfield, where temperature changes drastically, calibration precision is affected as a result. However, these problems could be solved if the constant temperature processing of the whole system is taken into consideration.

Table 6. Inversion Precision of Blackbody Radiance

Temperature of Blackbody (°C)	Theoretical Value of Radiance ($W \cdot m^{-2} \cdot sr^{-1}$)	Chosen Gear	Gray Value of Detector Element	Measured Value of Radiance ($W \cdot m^{-2} \cdot sr^{-1}$)	Measurement Error of Radiance (%)
120	0.2017	I	3709	0.2040	1.14
200	2.8294	II	5457	2.8575	0.99
170	1.1687	I	10012	1.1733	0.39
250	9.9721	III	3862	10.0703	0.98
230	6.1980	II	9651	6.2261	0.45
400	150.6898	IV	6103	152.7382	1.36
480	424.0013	V	3631	439.8743	3.74
550	900.7769	V	5434	916.6499	1.76
450	294.8251	IV	9988	297.4322	0.88
300	28.5559	III	7648	28.6541	0.34

REFERENCES

1. M. Ochs, A. Schulz, and H.-J. Bauer, "High dynamic range infrared thermography by pixelwise radiometric self calibration," Infrared Phys. Technol. **53**, 112–119 (2010).
2. T. Svensson, I. Renhorn, and P. Broberg, "Evaluation of a method to radiometric calibrate hot target image data by using simple reference sources close to ambient temperature," Proc. SPIE **7662**, 76620X (2010).
3. W. L. Wolfe, *Introduction to Radiometry* (SPIE, 1998).
4. P. W. Nugent, J. A. Shaw, and N. J. Pust, "Radiometric calibration of infrared imagers using an internal shutter as an equivalent external blackbody," Opt. Eng. **53**, 123106 (2014).
5. H. W. Yoon, G. P. Eppeldauer, and V. B. Khromchenkob, "Infrared collimator calibrations using regular glass optics and short-wave infrared detectors," Proc. SPIE **6940**, 694038 (2008).
6. M. E. Kaisera, J. W. Kruka, S. R. McCandliss, D. J. Sahnow, and B. J. Rauscher, "ACCESS: absolute color calibration experiment for standard stars," Proc. SPIE **7014**, 70145Y (2008).
7. J. T. McGraw, P. C. Zimmer, D. C. Zirzow, J. T. Woodward, K. R. Lykke, C. E. Cramer, S. E. Deustua, and D. C. Hines, "Near-field calibration of an objective spectrophotometer to NIST radiometric standards for the creation and maintenance of standard stars for ground- and space-based applications," Proc. SPIE **8450**, 84501S (2012).
8. G. T. Fraser, S. W. Brown, H. W. Yoon, B. C. Johnson, and K. R. Lykke, "Absolute flux calibrations of stars," Proc. SPIE **6678**, 66780P (2007).
9. C. Songtao, Z. Yaoyu, S. Zhiyuan, and L. Min, "Method to remove the effect of ambient temperature on radiometric calibration," Appl. Opt. **53**, 27, 6274–6279 (2014).
10. Y. Té, P. Jeseck, I. Pépin, and C. Camy-Peyret, "A method to retrieve blackbody temperature errors in the two points radiometric calibration," Infrared Phys. Technol. **52**, 187–192 (2009).
11. H. Lee, C. Oh, and J. W. Hahn, "Calibration of a mid-IR optical emission spectrometer with a 256-array PbSe detector and an absolute spectral analysis of IR signatures," Infrared Phys. Technol. **57**, 50–55 (2013).